A Novel Filter Rating Method Using Less Than 30-nm Gold Nanoparticle and Protective Ligand

Takehito Mizuno, Akihisa Namiki, and Shuichi Tsuzuki

***Abstract*—This paper describes a novel filter rating method beyond the current 30-nm limit by combining dynamic light scattering and inductively coupled plasma mass spectrometer technique and proposes the use of gold nanoparticle as the standard challenge particle. Furthermore, the effect of protective ligand addition is investigated in order to decrease the adsorbing effect between gold nanoparticle and membrane surface.**

***Index Terms*—Filters, gold, membranes, metals, particle measurements.**

I. Introduction

As SEMICONDUCTOR device design rules continue to shrink, particle contamination control becomes increasingly important, driven by ever decreasing critical particle sizes on Si wafers. Finer filters for various liquids are required to support increased demands outlined in the International Technology Roadmap for Semiconductors each year: now 30 nm and finer rated filters are critical for leading-edge semiconductor manufacturing facilities.

Fig. 1 shows the comparison of various membranes with regard to rating, particle sizing instrument, and standard challenge species. Despite microfiltration (MF) and ultrafiltration (UF) membranes' having already overlapped each other, different rating techniques are used. MF rating has been defined by particle removal efficiency using hard particles such as polystyrene latex (PSL) spheres. Meanwhile, UF rating is defined by challenging with some organics, including proteins and vitamins, using molecular weight cutoff concept [1]. Thus, there is no common indicator regarding particle removal capability between MF and UF membrane.

However, useful filter rating methods below 30 nm have not been reported. In general, filter ratings larger than 30 nm are typically defined by particle removal efficiency using laser light scattering particle counters and PSL as a standard challenge particle (test particle). But particle-counting technology has reached a limitation for particles less than 30 nm in size due to the very low counting efficiency at these small sizes. Also, PSL smaller than 20 nm has not been developed yet because of production difficulty. About six years ago, a filter rating method using fluorescence PSL was developed by using a fluorescence spectrophotometer instead of particle counters in order to improve detection sensitivity. However, the minimum particle size obtainable is basically equal to the conventional PSL one. Consequently, this method could not be applicable to a filter rating below 20 nm.

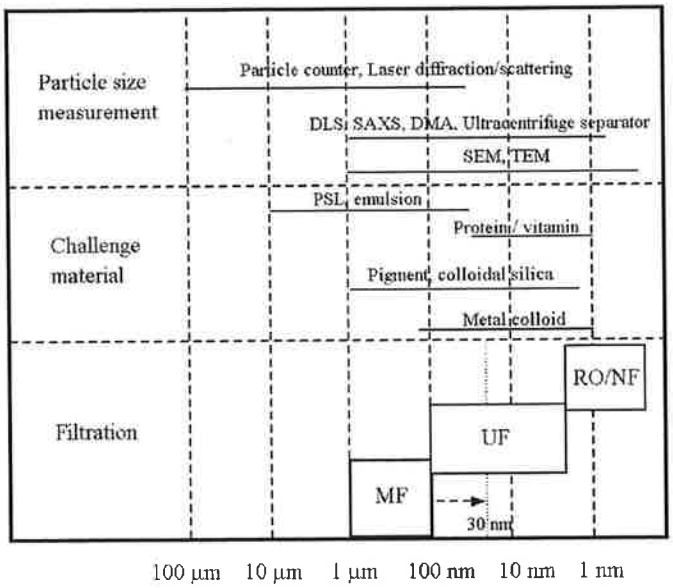

Fig. 1. Comparison of various membranes with regard to rating and standard challenge species. RO and NF means reverse osmosis and nanofiltration, respectively.

Generally, to make nanosized particles disperse stably in liquid phase is extremely difficult due to the reduction of electrostatic repulsion in proportion to particle size, as Derjaguin–Landau–Verway–Overbeek (DLVO) theory describes [2]. There are some nanosized rigid particles such as SiO_2, TiO_2, CeO_2, and precious metals, and whose sizes of primary particle nearly equal each catalog value by electron microscopy [3], [4]. But, almost all of the nanoparticles easily aggregate and create secondary particle or precipitation if there are disturbances such as concentration change, extraneous substance, pH fluctuation, and temperature change. Considering pros and cons of various particles, gold nanoparticle is adopted as the standard challenge particle because of the high stability, narrow particle size distribution, and roundness.

Gold nanoparticle is one of the oldest developed nanoparticles: it was originally used for stained glass beginning in about the seventeenth century [5], [6]. Faraday scientifically developed the synthesis method by using some chemicals in the nineteenth century [7]. Recently, precious-metal nanoparticles including gold nanoparticle has been expected for the purpose of microfabrication of thin films and line patterning as an alternate technique of plating.

Manuscript received April 15, 2009; revised August 11, 2009; accepted August 19, 2009. First published September 11, 2009; current version published November 04, 2009.

The authors are with the PI-Technology Division, Nihon Pall Ltd., Ibaraki 300-0315, Japan (e-mail: takehito_mizuno@ap.pall.com).

Digital Object Identifier 10.1109/TSM.2009.2031762

Other advantages of gold nanoparticle are as follows.

— About 1 nm to submicrometer particle sized gold particles are obtainable.
— It has been said that particle size distribution of gold nanoparticle less than 30 nm is narrower than that of PSL.
— High density of electrons causes high detectivity using optical methodology.
— Gold nanoparticle is harmless and nontoxic.

According to DLVO theory, it is expected that the aggregation and/or precipitation of colloidal nanoparticles easily occurs because their surface zeta potentials decrease in proportion to the particle size [2], [3], [8]. Thus, to monitor the particle size of challenged colloidal suspension is indispensable for accurate measurement of the filter's particle removal capability.

There are some instruments determining particle size in nanosized colloidal suspensions. Especially, small-angle X-ray scattering (SAXS), differential mobility analyzer (DMA), ultracentrifuge separator, and dynamic light scattering (DLS) are widely used. SAXS is often used to determine the crystalline particle size and structure by analyzing the scattered X-ray intensity in small angle. The particle size as intensity-weighted mean can be obtained by Guinier plot [9]. Since the wavelength of X-ray is generally smaller than the diameter of a colloidal particle, it is preferable to analyze nanoparticles [10]. However, X-ray intrinsically tends to penetrate into various materials and has very low scattering capability, especially against low-density materials such as PSL and colloidal silica. Thus, relatively highly concentrated (more than 5 wt%) samples are needed to detect sufficient scattered X-ray intensity and calculate accurate particle size data. Meanwhile, small-angle neutron scattering (SANS) is a similar technique to SAXS. DMA plays an important role in sizing of aerosol involving a particle larger than sub-10 nm [11]–[13].

Recently, some colloidal particles dispersed in liquid have been applied by vaporizing. But the particle size of gas phase is possibly different from that of liquid phase because aggregation or dispersion may occur in the phase transition from liquid to gas. Ultracentrifuge separator method is used with a scanning absorption optical system such as ultraviolet/visible (UV/VIS) in bioindustry for the purpose of protein separation and determination of particle size [14]. The resolution of determined particle size distribution is high in angstrom order if dense colloidal suspension is measured. However, the detection limit is relatively high due to the usage of UV/VIS, which needs a condensed sample. DLS, also named quasi-elastic light scattering or photon correlation spectroscopy, is the established instrument for the particle size measurement of colloidal particles in the range of about 1 nm to a few micrometers by in situ analyzing the fluctuation of the scattered light from colloidal particles [15]–[22]. The detection limit is relatively low. For instance, in the case of a 20-nm-sized particle, DLS can detect at the concentration on the order of a few parts per billion. Considering the pros and cons of the above four instruments, a DLS instrument was adopted because of its high sensitivity, short measurement time, and in situ measurement in liquid phase.

Inductively coupled plasma mass spectrometer (ICP-MS) technique is adopted as an alternative method of determining quantity to particle counter because a nanosized metal particle is used as a standard challenge particle and ICP-MS has the highest sensitivity of diluted metals. The particle counter has a fatal problem to detect even fine bubbles and contamination in liquid as if they were real particles. However, the ICP-MS instrument can only detect the used gold nanoparticle because the contamination of gold element is negligibly small, and this method can demonstrate accurate particle removal efficiency.

Hence, we investigated alternative techniques and concluded that combining DLS and ICP-MS with gold nanoparticle, as a challenge contaminant, was effective.

A challenge particle size below 30 nm in colloidal solution could be in situ measured with DLS, and it enables us to confirm the real particle size distribution and whether or not the colloidal system is stable. Thus, ICP-MS could measure concentrations of challenged gold nanoparticle in upstream and downstream with a high detectivity. Additionally, adding protective ligands for reducing the adsorbing effect between particle and membrane surface was examined and the mechanism of the repulsive force investigated.

II. Experimental

A. Gold Nanoparticle

Gold nanoparticles (EMGC series, 5, 10, 20 ,and 30 nm) supplied by British Biocell international, U.K., were suspended in dilutions of deionized water to test for efficacy as standard challenge particles. In order to prevent them from aggregating and decrease the adsorbing effect between the gold nanoparticle and the high-density polyethylene (HDPE) and nylon6,6 membrane surfaces, protective ligands (stabilizer), mercaptosuccinic acid (97%, Wako, Japan), and 2-amino-2-hydroxymethyl-1,3-propanediol (Wako, Japan), were used, respectively. Also, 3-mercaptopropionic acid, 2-mercaptopropionic acid, mercaptoacetic acid, and p-mercaptobenzoic acid were used to investigate the mechanism of adsorbing effect between gold nanoparticle and the HDPE membrane surface by comparing particle removal efficiencies. For nylon6,6 membrane, 3-mercapto-1,2-propanediol, 2-mercaptoethanol, 1-mercapto-2-propanol, 3-mercapto-1-propanol, 2-amino-2-methyl-1,3-propanediol, 2-amino-2-methyl-1-propanol, 2-amino-1,3-propanediol, 3-amino-1,2-propanediol, (R)-(−)-2-amino-1-propanol, and (S)-(+)-2-amino-1-propanol were used.

As a reference, 33 nm PSL, 3030A, supplied by Duke Scientific, was also used in challenging these membranes.

B. Membrane

Polytetrafluoroethylene (PTFE) membranes of UltiKleen Excellar ER (filter rating 20 nm, Pall) filter and UltiKleen Excellar (filter rating 30 nm, Pall) filter were used. Instead of a particle challenge test, ratings of 20 nm were estimated by extrapolation of the linear relationship between KL value—the critical pressure where isopropylalcohol (IPA) liquid film separated from the membrane pore—and reciprocal number of rating in the range of 30–200 nm, obtained by challenge testing as shown in Fig. 2. HDPE membranes of PE-Kleen UG001 (filter rating 10 nm, Pall) filter and UG003 (filter rating 30 nm, Pall) filter, nylon6,6 membranes of Ultipleat P-Nylon ANM (filter rating

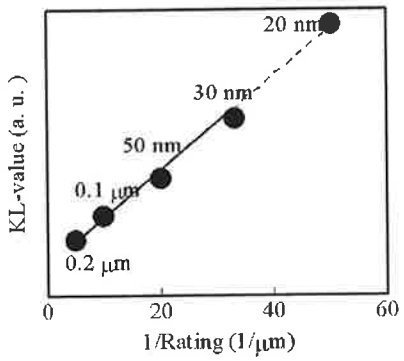

Fig. 2. Correlation between KL-value and 1/(rating) of various PTFE filters.

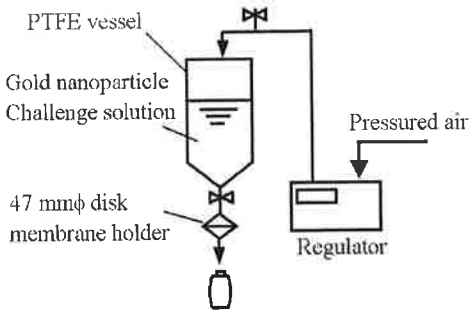

Fig. 3. Schematic drawing of the filter evaluation apparatus using 47 mm ϕ disk membrane.

20 nm, Pall) filter, and (filter rating 40 nm, Pall) filter were also used for the proposed evaluation. Each membrane was cut into 47-mm-diameter disks, and the filtration was performed by challenging with gold nanoparticle suspension after prewetting the membrane with IPA at a flow rate of 5 ml/min, corresponding approximately to 10 L/min when using a 10-in cartridge. Schematic drawing of the filtration apparatus is shown in Fig. 3. The challenge solution dispersed with gold nanoparticle was pressurized by regulated air and sent to the membrane holder.

C. Characterization

1) Particle Size Determination: DLS and Electron Microscopy: Particle size distributions of challenge gold nanoparticles were measured with DLS (Zetasizer Nano ZS, Malvern, U.K.) installed with a semiconductor laser operating at 532 nm and at an output power of 50 mW. The scattered light from the Brownian suspended particles was detected with an avalanche photodiode at the fixed back-scattering angle of 173°. The temperature of the sample cell holder was maintained constant at 296 K with a peltiert device. Analyzing the time-correlation function originating from the fluctuation of the scattered light, the diffusion coefficient D can be obtained by using the nonnegative least squares method. Then, hydrodynamic diameter d is calculated by following the Stokes–Einstein equation using solvent viscosity (η),

$$d = kT/(3\pi\eta D) \tag{1}$$

where k is Boltzmann's coefficient and T is absolute temperature in kelvin.

For comparison, electron microscopy observation was carried out with in-lens field emission scanning electron microscopy (FE-SEM) (S-5200, Hitachi, Japan), which could observe without the deposition of conductive material such as gold and carbon. Thus, the accurate size and shape of original gold nanoparticle could be demonstrated. The particle size distributions were determined by counting more than 100 particles. Gold nanoparticle suspensions were dropped on Si wafer, and the wafer sample was dried at room temperature for 24 h.

Transmission electron microscopy (TEM) observation was also carried out to elucidate the crystalline structure of 5 nm gold nanoparticle with high-resolution TEM (H-9000UHR, Hitachi, Japan) at an accelerating voltage of 300 kV.

2) Zeta Potential Measurement: Zeta potential is the electric potential difference between the bulk of solvent and ionic diffusion layer of fluid attached to the dispersed particles. The surface zeta potential of dispersed particle in liquid is one of the indexes predicting the stability of aqueous colloidal suspensions. If the zeta potential is more than 30 mV or less than −30 mV, the repulsive force is induced between suspended particles, which increases electrical repulsive force and the suspension stability. On the other hand, if the absolute value of zeta potential decreases less than about 30 mV, colloidal particles become unstable and aggregation occurs. The surface zeta potential of gold nanoparticle was obtained from the electrophoresis mobility using the optional function of the DLS instrument. Phase analysis light scattering and mixed mode measurement methods were used for eliminating the effect of electroosmotic flow. The zeta potential z was calculated using Henry equation

$$U_E = 2z\varepsilon f(Ka)/3\eta \tag{2}$$

where U_E means electrophoretic mobility and ε and η are dielectric constant and solvent viscosity, respectively. Since the gold nanoparticles were dispersed in water, then Henry coefficient $f(Ka)$, was set to 1.5 by applying Smoluchowski approximation.

3) Quantity Determination of Challenge Gold Nanoparticle: The quantity of gold in the feed and filtrate solution was determined with ICP-MS (HP-4500, Agilent Technologies). In order to make a calibration curve, gold standard solution ($HAuCl_4$, Wako, Japan) was used.

III. Results and Discussion

A. Particle Size Distribution

Fig. 4 shows the particle size distributions of 10-, 20-, and 30-nm gold nanoparticles measured with (a) DLS and (b) in-lens FE-SEM. PSL (33 nm) result by DLS is also shown in Fig. 4(a). FE-SEM images of the gold nanoparticles are shown in Fig. 5. The sizes of each challenge material are roughly the same, and the mean diameters of gold nanoparticle and PSL determined by DLS measurement were 11.3, 21.6, 30.7, and 32.5 nm, respectively. The distribution of the PSL was a little broader than the gold nanoparticles. From the FE-SEM observation, the average particle size of 10, 20, and 30-nm gold nanoparticles was 8.6,

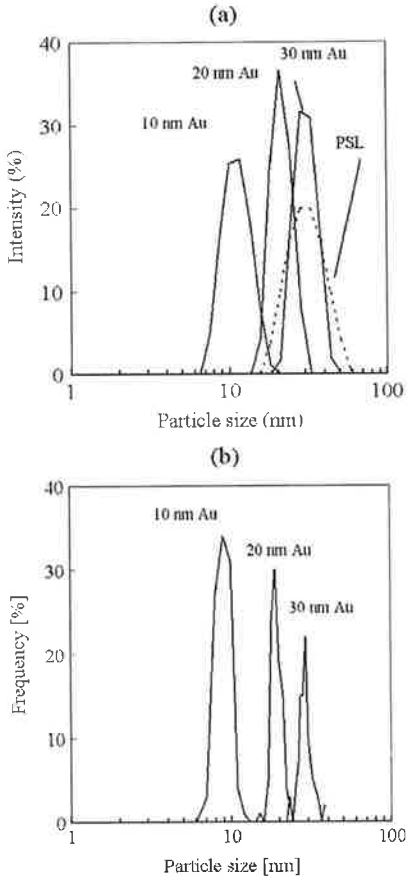

Fig. 4. Particle size distributions of 10-, 20-, 30-nm gold nanoparticle and 33 nm PSL measured with (a) DLS and (b) in-lens FE-SEM except PSL (shown in Fig. 5).

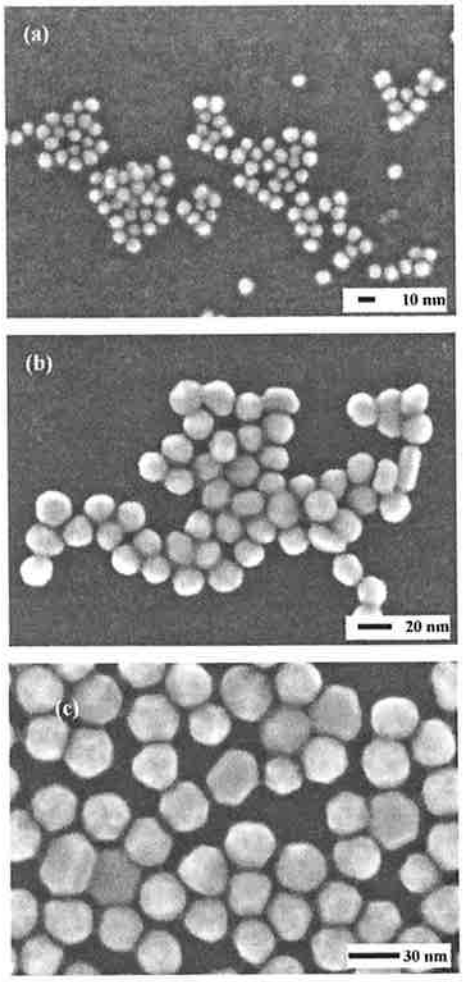

Fig. 5. In-lens FE-SEM images of the (a) 10-, (b) 20-, and (c) 30-nm gold nanoparticles. Since no deposition such as Pt, Au, and carbon is conducted, the increase of particle size is not expected.

18.8, and 28.6 nm, respectively. According to the National Institute of Standards and Technology (NIST), 10-nm gold nanoparticle supplied by British Biocell International was certified as reference material. NIST has released the average particle size of 10-nm gold nanoparticle (RM8011) as 9.9 ± 0.1 nm by SEM and 13.5 ± 0.1 nm by DLS, and also has released the 30-nm result (RM8012) as 26.9 ± 0.1 nm by SEM and 28.6 ± 0.9 nm by DLS. Table I summarizes these results, including the NIST report. In general, the particle size of DLS is larger than that of electron microscopy because DLS measures the hydrodynamic diameter of the colloidal particle covered with molecules, ions, and solvent.

B. 30-nm Gold Nanoparticle Versus 33 nm PSL Challenge Test

Fig. 6 indicates the removal efficiencies of Excellar ER (20 nm) membrane versus total particle concentration using the 30-nm gold nanoparticle and 33 nm PSL. Removal efficiencies by both have nearly the same values, which are asymptotically close to 100% in the measured range.

Thus, the proposed rating method using 30-nm gold nanoparticle showed equivalent removal efficiency for 20-nm PTFE filter as compared to the conventional rating method using 33-nm PSL.

C. Evaluation of the Excellar and Excellar ER PTFE Membrane

Fig. 7 shows the result of applying the proposed method to Excellar ER membrane estimated as 20 nm by KL extrapolation method (Fig. 1) using 0.5 ppm (3.5E+9 pcs/ml) suspension of 20-nm gold nanoparticle, with the particle size confirmed as shown in Figs. 2 and 3. Filter membranes of 30 nm rating showed lower removal efficiency, while the Excellar ER (20 nm) membrane shows more than 99% removal efficiency, as expected based on the membrane design.

D. Effect of Ligand Addition for the Reduction of Adsorbing Effect

Gold nanoparticle is generally prepared by the reduction of chloraulic acid ($HAuCl_4$) with citric acid physically adsorbed to the surface of gold and makes gold electrically stable in water [5], [6], [23]. As PTFE has very low surface energy, no interaction between the gold nanoparticle and the PTFE surface is expected. However, higher than expected particle removal efficiency might be found when challenging HDPE and nylon6,6 membranes due to surface interactions. In other words, these membranes could trap particles by adsorbing effect as well as

TABLE I
SUMMARY OF COMPARISON OF PARTICLE SIZE BY DLS AND TEM. THE RESULT REPORTED BY NIST ALSO IS DESCRIBED

Sample	DLS (nm)	FE-SEM (nm)	DLS by NIST (nm)	SEM by NIST (nm)
10 nm gold	11.3	8.6	13.5	9.9
20 nm gold	21.6	18.8	-	-
30 nm gold	30.7	28.6	28.6	26.9
33 nm PSL	33.5	-	-	-

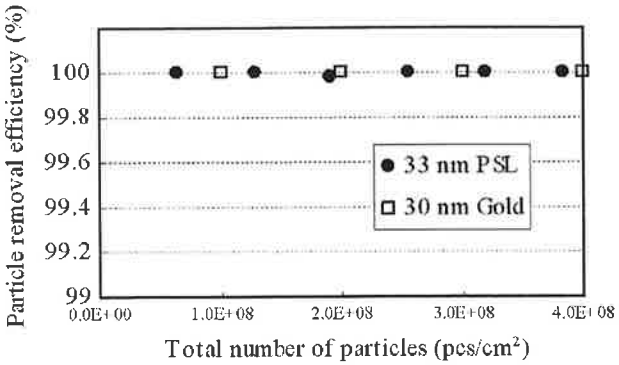

Fig. 6. Particle removal efficiencies of Excellar ER (20 nm) membrane by 30-nm gold nanoparticle and 33-nm PSL as a function of challenged particle concentration.

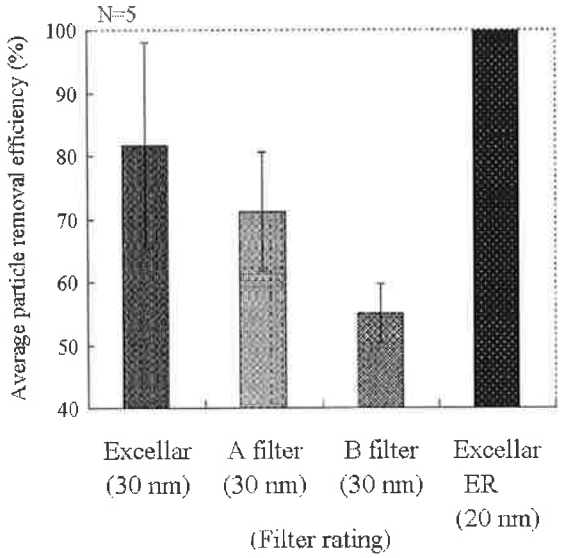

Fig. 7. Average particle removal efficiencies of PTFE membranes measured using 20-nm gold nanoparticle shown in Figs. 4 and 5. Challenge particle concentration is 0.5 ppm (= 3.5E + 9 pcs/ml).

filtration. Generally, almost all filters trap particles by both filtration and adsorption, but the adsorption in intensity highly depends on the properties of liquid, particle, and membrane surface. The ideal function of filter is to catch particles by only the filtrate function even at the condition of no adsorption effect expected. Actually, there are many kinds of particles and fluids at real filtration field, and thus gold nanoparticle and conventional PSL in deionized water (DIW) cannot always be the model particle representing these countless particles. But it is very important to prove the particle removal capability even when nonadsorbing particle comes to filter. Meanwhile, in the challenge test using PSL, Triton X-100 as surfactant is also used in order to decrease the removal efficiency [24], [25]. Hence, some protective ligands were investigated to reduce the attractive force between nanoparticle and membrane.

It is well known that the precious metal surface selectively adsorbs sulfur and nitrogen [26]–[36] and has a strong binding energy of Au-S estimated to be about 170 kJ/mol [37]. Therefore, the gold surface can be easily modified by thiol or amino functional groups [38], [39], and various properties such as hydrophilic/hydrophobic and cationic/anionic can be added. Investigating some protective ligands, we concluded that mercaptosuccinic acid for HDPE and 2-amino-2-hydroxymethyl-1,3-propanediol for nylon6,6, respectively, are very effective for reducing particle adsorption and eventually effective for reducing higher than expected particle removal efficiency. Fig. 8 shows the result of particle removal efficiency with the addition of ligands to the gold nanoparticle dispersion liquid at the various concentrations noted. Without protective ligands, high removal efficiencies of all membranes were observed. For example, UG003 (rating = 30 nm) could trap 10-nm gold nanoparticle at nearly 100%. This result means that adsorbing effect is dominant at this condition. On increasing the concentration of the ligands, the particle removal efficiencies of (b) UG003 (30 nm) and (d) AND (40 nm) membranes were decreased and approached certain values. On the contrary, (a) UG001 (10 nm) and (c) ANM (20 nm) membranes have high removal capability even when challenging gold nanoparticle with a dense ligand concentration. Thus, this result means that UG001 and ANM have high filtration removal capability against 10- and 20-nm particles, respectively, without adsorbing effect.

E. Mechanism of the Reduction of Adsorbing Effect by Adding Protective Ligands

DLVO theory, accomplished in the middle of the twentieth century [2], describes aggregation/dispersion phenomenon regarding van der Waals interaction and electrostatic repulsion originated from double layer force. Electrostatic repulsion force, so-called zeta potential, needs to be increased to obtain a stably dispersed colloidal system. Absolute value of zeta potential is well known to be proportional to the particle size d_P as following repulsive potential using Debye–Huckel approximation

$$V_R = 32kTn_0d_P\gamma^2\exp(-\kappa h)/\kappa^2 \propto d_P \tag{3}$$

where k is Boltzmann's constant. n_0 and γ are the number density of ion in the bulk solution and the reduced surface potential, respectively. $1/\kappa$ and h are the Debye length, the thickness

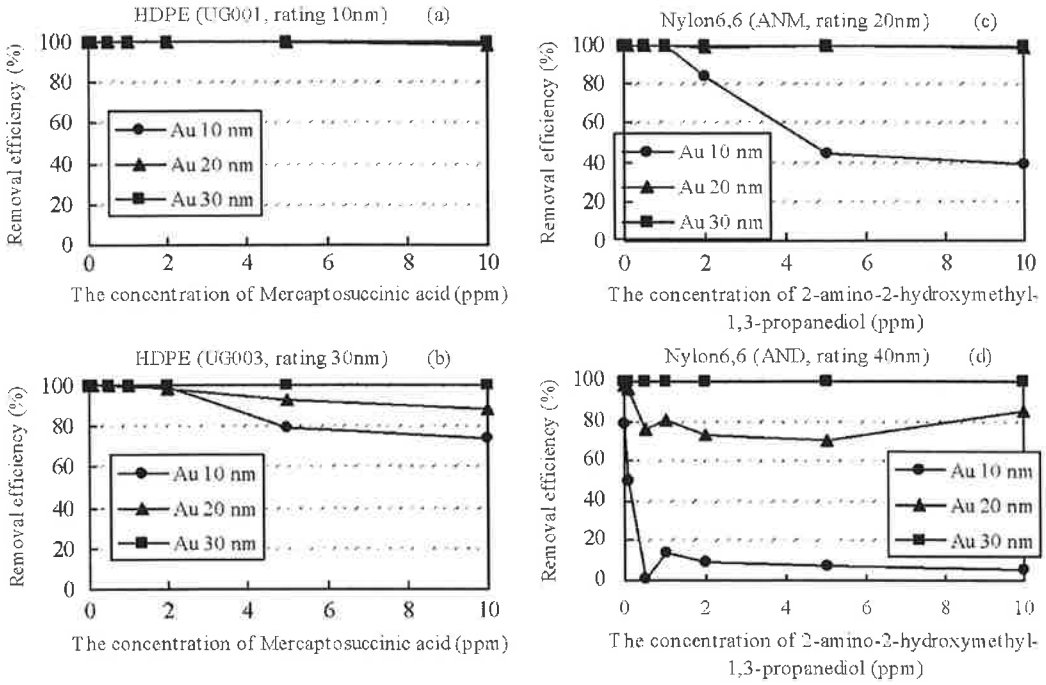

Fig. 8. Particle removal efficiencies of polyethylene and nylon6,6 against 10-, 20-, and 30-nm gold nanoparticle with protective ligands.

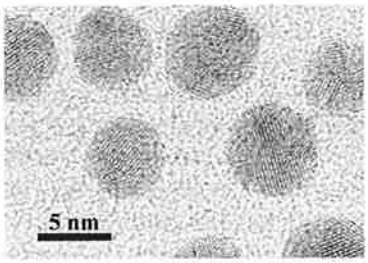

Fig. 9. High-resolution TEM image of 5-nm gold nanoparticle dried on Si wafer without protective ligand. Some crystalline facets are observed. S- and N-elements could combine with the surface elements of gold nanoparticle.

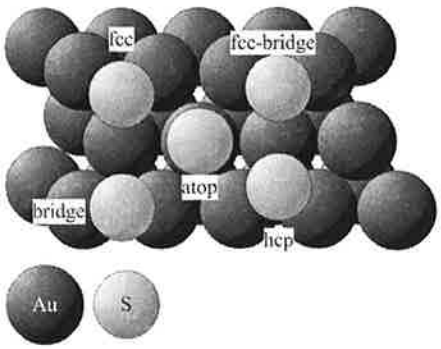

Fig. 10. Schematic illustration of S- or N-element possible adsorption site on the Au (111) surface. The most stable site is expected to be atop or bridge site.

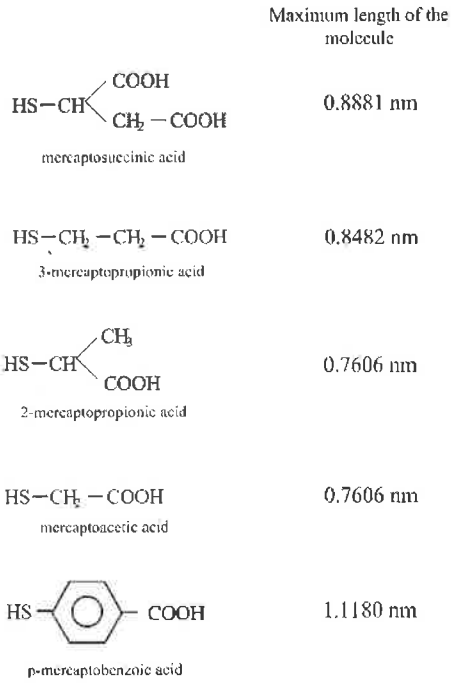

Fig. 11. Molecular structure of ligands used for HDPE membrane to examine the adsorbing effect.

of electrostatic double-layer, and a distance between interfacial particles.

The smaller the particle size is, the smaller the absolute value of zeta potential is, and therefore aggregation and sedimentation easily occur. The gold nanoparticle used in this paper is uniformly covered by citric acid, which can electrostatically and physically stabilize colloidal system. Even if the gold nanoparticles are stably dispersed in liquid phase, they tend to adsorb on the membrane surface due to low freedom of motion.

The van der Waals attractive interaction energy between sphere particle and surface is theoretically describes as follows:

$$\text{particle-surface} \quad V_{\text{vdw}} = H_A d_P / 6h \tag{4}$$

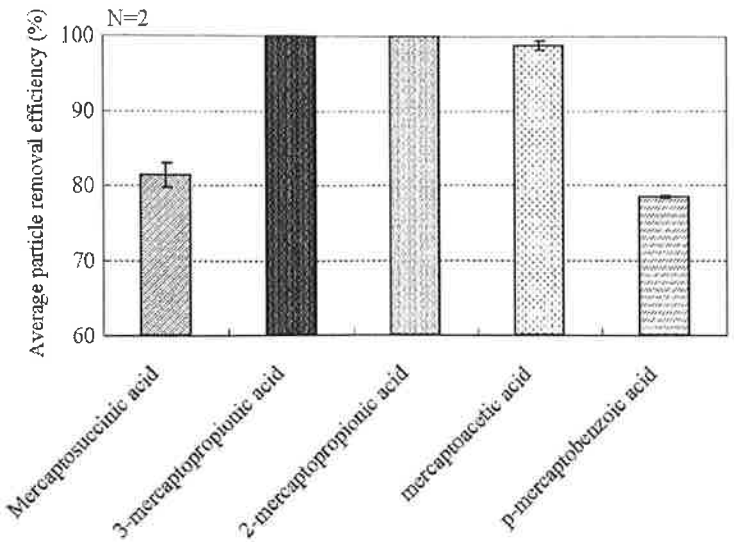

Fig. 12. Average particle removal efficiencies of 30 nm rating of HDPE membrane against 10-nm gold nanoparticles covered with various ligands. Challenge particle concentration is 0.5 ppm (= 2.85E + 10 pcs/ml); ligand concentration is 0.1 mmol/l.

where H_A is the Hamaker constant. H_A is dependent to some degree on the electronic density of the particle and surface and the solvent intervening between particle and surface. Particularly, the H_A value in the case of PTFE membrane is smaller than that of other resins. Therefore, the adsorbing effect between particle and PTFE surface could be ignored. On the other hand, HDPE and nylon6,6 membranes have relatively high H_A; thus particles could easily adsorb on their membrane surfaces.

In the previous section, some specific protective ligands have an effect on decreasing adsorbing effect. The mechanism of the reduction of adsorbing effect was examined by comparing some protective ligands in regard to chain length and straight/branch chain. Meanwhile, Triton X-100 as non-ion surfactant has been used for PSL particle challenge test in order to decrease adsorbing effect. It can decrease the attractive interaction between particle and membrane by the steric effect as one of the non-DLVO forces [24], [25].

A TEM image of 5 nm gold nanoparticle is shown in Fig. 9. Gold is well known as a face-centered cubic lattice (FCC) crystal; thus some ordered crystalline facets are observed. Thiol (SH) and NH_2 could combine with Au element at bridge or atop site with a kind of covalent bond, as shown in Fig. 10 [39]–[41], and produce the self-assembled monolayer (SAM)-like Langmuir-type adsorption on the gold surface [42], [43]. Furthermore, Petri showed evidence that the second layer can be made on the first SAM by the driving force of the intermolecular hydrogen bonds [44]. Also, Nara reported that the ligand combining with Au element could change the bond angle [45].

HDPE membrane, which has a rating of 30 nm, was challenged with the 10-nm gold nanoparticle covered with mercaptosuccinic acid, 3-mercaptopropionic acid, 2-mercaptopropionic acid, mercaptoacetic acid, and p-mercaptobenzoic acid to examine the influence of molecular structure by varying with molecular length, straight/branch chain, and functional group. Schematic drawings of each protective ligand with maximum length of the molecule are shown in Fig. 11. As a result, mercaptosuccinic acid and p-mercaptobenzoic acid could decrease the particle removal efficiency to the same degree as shown in Fig. 12. The hydrodynamic diameters and zeta potential of each 10-nm gold nanoparticle treated with each protective ligand are summarized in Table II. Although the zeta potentials are maintained almost constant below −25 mV except 2- and 3-mercaptopropionic acids, the particle size is greatly varied due to the ligand adsorption on the particle surface. Table II also indicates the calculated hydrodynamic diameter considering the first and second layer of protective ligands. These actual hydrodynamic diameters measured with DLS may represent the second layer except 2- and 3-mercaptopropionic acids.

In Fig. 13, schematic drawings of the atomic configurations of straight and branched chain structure of protective ligands (3-mercaptopropionic acid and mercaptosuccinic acid) are shown. A branched or bulky protective ligand has a structure of thick chain and tends to create the perpendicular structure to gold surface due to the physical closeness and each repulsive interaction force of the neighboring ligand. On the other hand, straight chain ligand has a lot of freedom in geometry and could tilt the chain structure, as shown in Fig. 13. Accordingly, the gold nanoparticle covered with bulky ligand, which has a long chain and branched/bulky structure, tends to have a large hydrodynamic diameter and physically restrain the gold nanoparticle from approaching the membrane surface. Templeton reported the difference of reactivity comparing various ligands bonded on the surface of gold and concluded the steric effect caused the affect of reactivity [43].

Thus, the gold nanoparticle treated with a straight chain ligand could approach the membrane surface more closely than a branched or bulky ligand and have a high possibility to adsorb. Consequently, the reduction of particle removal efficiency is mainly caused by the steric effect as non-DLVO force. However, the particle removal efficiency of the particle covered with 2-mercaptopropionic acid is still high in spite of the large hydrodynamic diameter. The reason for high removal efficiency is not clear, but the branched methyl group may

TABLE II
PARTICLE SIZE (HYDRODYNAMIC DIAMETER) AND ZETA POTENTIALS MEASURED WITH DLS ADDING VARIOUS LIGANDS TO 10-nm GOLD NANOPARTICLE FOR HDPE MEMBRANE

Ligand	Particle size (nm)	Zeta potential (mV)	Expected particle size by first-layer adsorption (nm)	Expected particle size by second-layer adsorption (nm)
mercaptosuccinic acid	14.6	-33.8	13.1	14.9
3-mercaptopropionic acid	11.5	-27.2	13.0	14.7
2-mercaptopropionic acid	14.9	-40.5	12.8	14.4
mercaptoacetic acid	13.3	-35.3	12.8	14.4
p-mercaptobenzoic acid	16.4	-27.1	13.6	15.8

Expected particle sizes are calculated by using maximum length of molecule shown in Fig. 11 and the particle size of 10 nm gold nanoparticle written in Table I. Zeta potentials measurements were conducted with 20 nm gold nanoparticle due to the lack of the scattered intensity from 10 nm gold nanoparticle.

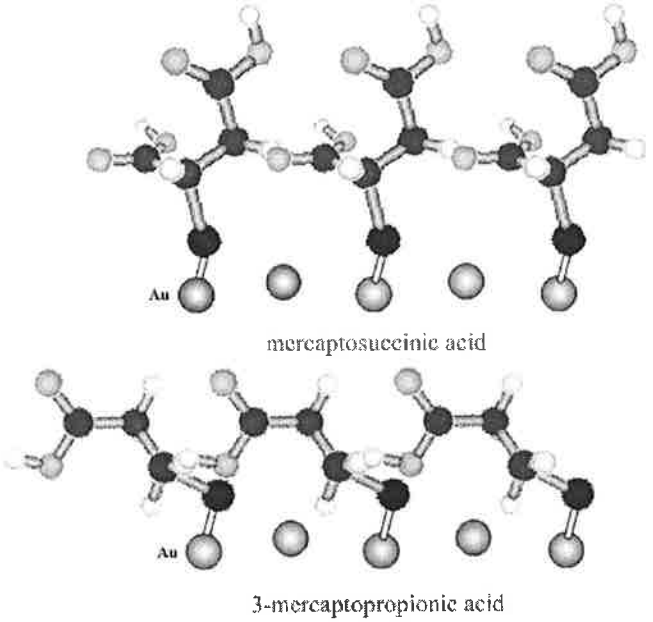

Fig. 13. Schematic drawing of atomic configurations of straight and branched chain structure of protective ligands combining with Au element (3-mercaptopropionic acid and mercaptosuccinic acid).

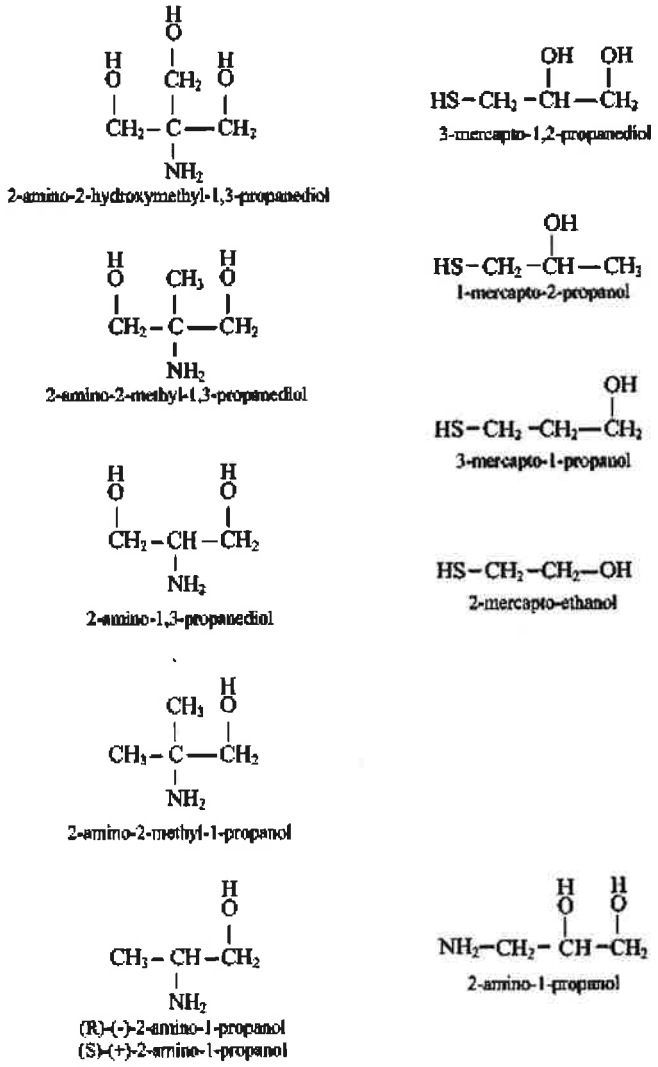

Fig. 14. Schematic drawing of ligands used for nylon6,6 membrane to examine the mechanism of adsorbing effect.

have a hydrophobic attractive interaction with the polyethylene group. Thus, an investigation of the membrane surface would be needed using atomic force microscopy or another technique.

Nylon6,6 membrane, which has a rating of 20 nm, was challenged with the 10-nm gold nanoparticle treated with various ligands that have a thiol group or amino group; protective ligands are 3-mercapto-1,2-propanediol, 2-mercaptoethanol, 1-mercapto-2-propanol, 3-mercapto-1-propanol, 2-amino-2-methyl-1,3-propanediol, 2-amino-2-methyl-1-propanol, 2-amino-1,3-propanediol, 3-amino-1,2-propanediol, (R)-(−)-2-amino-1-propanol, and (S)-(+)-2-amino-1-propanol. The purpose of using their protective ligands is to examine the root cause of reduction of adsorbing effect; which element of S and N is effective; or which end-group and end-structure is effective. Schematic drawings of these protective ligands are shown in Fig. 14. Particle challenge test results using these ligands are summarized in Fig. 15. The particle removal efficiencies of all the ligands including thiol group were extremely high. This means the nylon6,6 membrane adsorbed the gold nanoparticles combining thiol group. On the other hand, the particle removal efficiencies of all the ligands including amino group were lower than 60%. The hydrodynamic diameters of 10-nm gold nanoparticle and zeta potential of 20 nm treated with each protective ligand are summarized in Table III.

Therefore, the NH group in nylon6,6 molecular structure probably has the repulsive force against the amino group in ligand, which directly combines with the gold surface. It seems that outer molecular structure in ligands such as methyl and alcohol group does not have any effect on the interaction with nylon6,6 membrane.

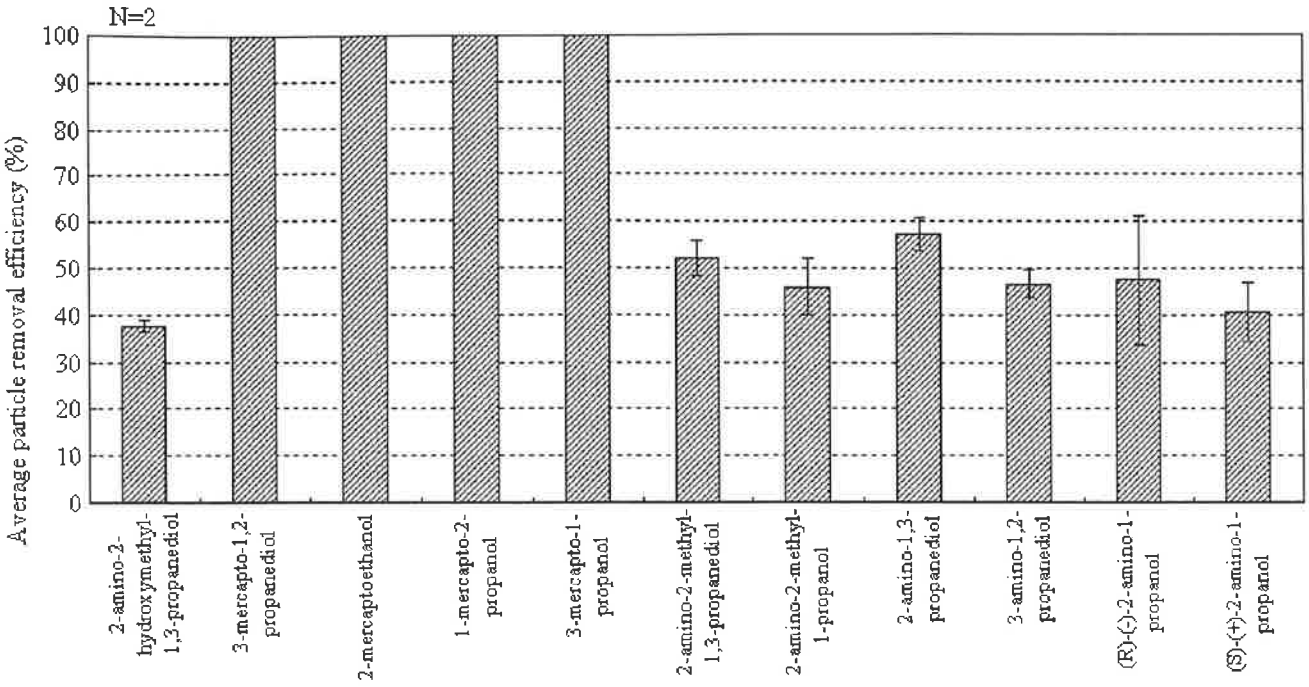

Fig. 15. Average particle removal efficiencies of nylon6.6 membrane against gold nanoparticles covered with various ligands. 20 nm rating of nylon6.6 membranes was challenged with 10-nm sized gold nanoparticle treated with various ligands. Challenge particle concentration is 0.5 ppm (= 2.85E + 10 pcs/ml); ligand concentration is 0.1 mmol/l.

TABLE III
PARTICLE SIZE (HYDRODYNAMIC DIAMETER) AND ZETA POTENTIALS MEASURED WITH DLS ADDING VARIOUS LIGANDS TO 10-nm GOLD NANOPARTICLE FOR NYLON6,6 MEMBRANE

Ligand	Particle size (nm)	Zeta potential (mV)
2-amino-2-hydroxymethyl-1,3-propanediol	14.6	-39.8
3-mercapto-1,2-propanediol	13.0	-24.3
2-mercaptoethanol	26.1	-12.0
1-mercapto-2-propanol	10.4	-30.7
3-mercapto-1-propanol	227.9	-13.5
2-amino-2-methyl-1,3-propanediol	12.1	-23.0
2-amino-2-methyl-1-propanol	17.3	-36.8
2-amino-1,3-propanediol	13.0	-30.5
3-amino-1,2-propanediol	12.3	-17.2
(R)-(-)-2-amino-1-propanol	13.3	-24.5
(S)-(+)-2-amino-1-propanol	14.8	-27.7

Zeta potentials measurements were conducted with 20 nm gold nanoparticle due to the lack of the scattered intensity from 10 nm gold nanoparticle.

IV. CONCLUSION

We developed a new rating method for filters finer than 30 nm by combining DLS and ICP-MS instrumentation with gold nanoparticle as a standard challenge suspension. Consequently, actual performance in terms of particle removal efficiency for rated membranes finer than 30 nm was demonstrated. DLS results regarding particle size distributions show good agreement with the result from in-lens FE-SEM observation. Additionally, some protective ligands were proven to be significant in order to reduce the particle-membrane attractive interaction.

REFERENCES

[1] R. W. Baker, *Membrane Technology and Applications*. London, U.K.: McGraw Hill, 1999.
[2] J. N. Israelachvili, *Intermolecular and Surface Forces*. New York: Academic, 1992.
[3] G. Schmid, *Nanoparticles—From Theory to Application*. Berlin, Germany: Wiley-VCH, 2004.
[4] Y. J.-N. and J. R. Lead, "Manufactured nanoparticles: An overview of their chemistry, interactions and potential environmental implications," *Sci. Total Environ.*, vol. 400, pp. 396–414, 2008.
[5] M.-C. Daniel and D. Astruc, "Gold nanoparticles: Assembly, supramolecular chemistry, quantum-size-related properties, and applications toward biology, catalysis, and nanotechnology," *Chem. Rev.*, vol. 104, pp. 293–346, 2004.
[6] T. Nagaoka, H. Shiigi, and S. Tokonami, "Highly sensitive and selective chemical sensing techniques using gold nanoparticle assemblies and superstructures," *Bunseki Kagaku*, vol. 56, no. 4, pp. 201–211, 2007.
[7] M. Faraday, "Experimental relations of gold (and other metals) to light," *Phil. Trans. Roy. Soc.*, vol. 147, pp. 145–181, 1857.
[8] T. Mizuno, A. Namiki, S. Tsuzuki, and T. Numaguchi, "A novel filter rating method for less than 30 nm particle," in *Proc. Conf. 17th Int. Symp. Semicond. Manuf.*, 2008, pp. 361–364.
[9] A. Guinier and G. Fournet, *Small-Angle Scattering of X-Rays*. New York: Dover, 1957.
[10] O. Glatter and O. Kratky, *Small-Angle X-Ray Scattering*. New York: Academic, 1982.
[11] J. R.-L., . I. G. Loscertales, D. Bingham, and J. Fernandez de la Mora, "Sizing nanoparticles and ions with a short differential mobility analyzer," *J. Aerosol Sci.*, vol. 27, no. 5, pp. 695–719, 1996.
[12] D. Hummes, S. Neumann, H. Fissan, D. R. Chen, D. Y. H. Pui, F. R. Quant, and G. J. Sem, "Nanometer differential mobility analyzer (nano-DMA): Experimental evaluation and performance verification," *J. Aerosol Sci.*, vol. 27, pp. S135–S236, 1996, Suppl. 1.
[13] J. F. de la Mora, L. de Juan, T. Eichler, and J. Rosell, "Differential mobility analysis of molecular ions and nanometer particles," *Trends Anal. Chem.*, vol. 16, no. 6, pp. 328–339, 1998.
[14] H. Colfen and T. Pauck, "Determination of particle size distributions with angstrom resolution," *Coll. Polymer Sci.*, vol. 275, pp. 175–180, 1997.
[15] B. J. Berne and R. Pecora, *Dynamic Light Scattering With Applications to Chemistry, Biology, and Physics*. New York: Dover, 2000.
[16] H. C. van de Hulst, *Light Scattering by Small Particles*. New York: Dover, 1981.
[17] J. Holoubek, "Some applications of light scattering in materials science," *J. Quant. Spec. Rad. Trans.*, vol. 106, pp. 104–121, 2007.
[18] D. G. Dalgleish and F. R. Hallett, "Dynamic light scattering: Applications to food systems," *Food Res. Inter.*, vol. 28, no. 3, pp. 181–193, 1995.

[19] P. N. Pusey and R. J. A. Tough, "Dynamic light scattering, a probe of Brownian particle dynamics," *Adv. Coll. Inter. Sci.*, vol. 16, pp. 143–159, 1982.
[20] R. Finsy, "Particle sizing by quasi-elastic light scattering," *Adv. Coll. Inter. Sci.*, vol. 52, pp. 79–143, 1994.
[21] K. Schatzel, "Light scattering—Diagnostic methods for colloidal dispersions," *Adv. Coll. Inter. Sci.*, vol. 46, pp. 309–332, 1993.
[22] P. Salgi and R. Rajagopalan, "Polydispersity in colloids: Implications to static structure and scattering," *Adv. Coll. Inter. Sci.*, vol. 43, pp. 169–288, 1993.
[23] J. Kunze, I. Burgess, R. Nichols, C. B. Herman, and J. Lipkowski, "Electrochemical evaluation of citrate adsorption on Au(111) and the stability of citrate-reduced gold colloids," *J. Electroanal. Chem.*, vol. 599, pp. 147–159, 2007.
[24] D. Elzo, Pchmitz, D. Houi, and S. Joscelyne, "Measurement of particle/membrane interactions by a hydrodynamic method," *J. Mem. Sci.*, vol. 109, pp. 43–53, 1996.
[25] J.-K. Lee, B. Y. H. Liu, and K. L. Rubow, "Latex sphere retention by microporous membranes in liquid filtration," *J. IES*, vol. 33, pp. 26–36, 1993.
[26] L. Pasquato, P. Pengo, and P. Scrimin, "Functional gold nanoparticles for recognition and catalysis," *J. Mater. Chem.*, vol. 14, pp. 3481–3487, 2004.
[27] T. Yonezawa, K. Yasui, and N. Kimizuka, "Controlled formation of smaller gold nanoparticles by the use of four-chained disulfide stabilizer," *Langmuir*, vol. 17, pp. 271–273, 2001.
[28] S. Chen and K. Kimura, "Synthesis and characterization of carboxylate-modified gold nanoparticle powders dispersible in water," *Langmuir*, vol. 15, pp. 1075–1082, 1999.
[29] S. Yagyu, M. Yoshitake, and T. Chikyow, "Adsorption structure and work function of succinic acid on Cu(110) surface," *Hyomen Kagaku*, vol. 28, no. 9, pp. 525–531, 2007.
[30] K. Motobayashi, C. Matsumoto, Y. Kim, and M. Kawai, "Surface dynamics of water monomers and dimers on Pt(111) surface," *Hyomen Kagaku*, vol. 28, no. 7, pp. 354–360, 2007.
[31] G. T. Hermanson, *Bioconjugate Techniques*. New York: Academic, 2008.
[32] N. Wangoo, K. K. Bhasin, S. K. Mehta, and C. Raman Suri, "Synthesis and capping of water-dispersed gold nanoparticles by an amino acid: Bioconjugation and binding studies," *J. Coll. Inter. Sci.*, vol. 323, pp. 247–254, 2008.
[33] G. Li, M. Lauer, A. Schulz, C. Boettcher, F. Li, and J.-H. Fuhrhop, "Spherical and planar gold(0) nanoparticles with a rigid gold(I)-anion or a fluid gold(0)-aceton surface," *Langmuir*, vol. 19, pp. 6483–6491, 2003.
[34] T. Kawano, Y. Horiguchi, Y. Niidome, T. Niidome, and S. Yamada, "Preparation of cationic gold nanoparticles in aqueous solutions of 2-aminoethanethiol hydrochloride," *Bunseki Kagaku*, vol. 54, no. 6, pp. 521–526, 2005.
[35] S. Diegoli, A. Manciulea, S. Begum, I. P. Jones, J. R. Lead, and J. A. Preece, "Interaction between manufactured gold nanoparticles and naturally occurring organic macromolecules," *Sci. Total Environ.*, vol. 402, pp. 51–61, 2008.
[36] S. I. Stoeva, A. B. Smetana, C. M. Sorensen, and K. J. Klabunde, "Gram-scale synthesis of aqueous gold colloids stabilized by various ligands," *J. Coll. Inter. Sci.*, vol. 309, pp. 94–98, 2007.
[37] J. B. Schlenoff, M. Li, and H. Ly, "Stability and self-exchange in alkanethiol monolayers," *J. Amer. Chem. Soc.*, vol. 117, pp. 12528–12536, 1995.
[38] M. J. Hostetler, A. C. Templeton, and R. W. Murray, "Dynamics of place-exchange reactions on monolayer-protected gold cluster molecules," *Langmuir*, vol. 15, pp. 3782–3789, 1999.
[39] H. Kondoh, M. Iwasaki, T. Shimada, and K. Amemiya, "Structure analysis of methylthiolate adsorbed on Au(111) by photoelectron diffraction," *Hyomen Kagaku*, vol. 24, no. 8, pp. 448–454, 2003.
[40] Y. Morikawa, T. Hayashi, C. C. Liew, and H. Nozoye, "First-principles molecular dynamics simulation of alkanethiol self-assembled monolayers on Au," *Hyomen Kagaku*, vol. 23, no. 7, pp. 423–430, 2002.
[41] D. C. Jackson, A. Chaudhuri, T. J. Lerotholi, D. P. Woodruff, R. G. Jones, and V. R. Dhanak, "The local adsorption site of methylthiolate on Au(111): Bridge or atop?," *Surface Sci.*, to be published.
[42] A. C. Templeton, W. P. Wuelfing, and R. W. Murray, "Monolayer-protected cluster molecules," *Acc. Chem. Res.*, vol. 33, pp. 27–36, 2000.
[43] A. C. Templeton, M. J. Hostetler, C. T. Kraft, and R. W. Murray, "Reactivity of monolayer-protected gold cluster molecules: Steric effects," *J. Amer. Chem. Soc.*, vol. 120, pp. 1906–1911, 1998.
[44] M. Petri, D. M. Kolb, U. Memmert, and H. Meyer, "Adsorption of mercaptopropionic acid onto Au(111) Part I. adlayer formation, structure and electrochemistry," *Electrochem. Acta*, vol. 49, pp. 175–182, 2003.
[45] J. Nara, S. Higai, Y. Morikawa, and T. Ohno, "Adsorption structure of benzenethiol on Au(111): First-principles study," *Appl. Surface Sci.*, vol. 237, pp. 433–438, 2004.

Takehito Mizuno received the B.S. and M.S. degrees in chemical engineering from Doshisha University, Kyoto, Japan, in 1998 and 2000, respectively.

He joined Hamamatsu Photonics K.K., Shizuoka, Japan, where he developed photodiode detectors; and Mitsui Co./XNRI, Tokyo, Japan, where he worked in research and development of inorganic zeolite membranes used for solvent dehydration and gas/gas separation. He is currently a Senior Engineer with the R&D Division, Nihon PALL Ltd., Tsukuba, Japan, where his work mainly involves the development of lower extractable filters and the measurement technique of filtrating performance of the most advanced filter. His current research interests are in nanoparticle and interface science, the mechanism of nanoparticle filtration, and pervaporation/gas separation.

Mr. Mizuno is a member of the Japan Society of Applied Physics and the Society of Chemical Engineers, Japan.

Akihisa Namiki received the bachelor's degree from Toyo University, Tokyo, Japan, in 1995 and the M.E. degree from Toyo University Graduate School of Engineering, Tokyo, in 1998.

He was a Process Engineer with SpeedFam-IPEC K.K., Kanagawa, Japan, and Novellus Systems Japan, Inc., Kanagawa, where he working on developing CMP process. He is currently a Senior Staff Scientist with the Scientific & Laboratory Services Division, Nihon Pall Ltd., Tsukuba, Japan, where he works on filtrations research regarding deionized water and chemicals in semiconductor, display, and HDD manufacture.

Mr. Namiki is a member of the Japan Society of Applied Physics and the Ceramic Society of Japan

Shuichi Tsuzuki received the bachelor's degree in applied chemistry from the Science University of Tokyo, Tokyo, Japan, in 1987.

He is now an ME Group Manager with the Scientific and Laboratory Services Division, Nihon Pall Ltd., Tsukuba, Japan.